EUSIPCO 2013 1569745717

ANALYTICAL EXPRESSIONS OF POWER SPECTRAL DENSITY FOR GENERAL SPECTRALLY SHAPED SC-FDMA SYSTEMS

*Bouchra Benammar**, *Nathalie Thomas**, *Marie-Laure Boucheret**, *Charly Poulliat** *and Mathieu Dervin*†

* University of Toulouse, INPT-ENSEEIHT/IRIT
† Thales Alenia Space, Toulouse
Email: {bouchra.benammar, nathalie.thomas, marie-laure.boucheret, charly.poulliat }@enseeiht.fr, mathieu.dervin@thalesaleniaspace.com

ABSTRACT

In this work, Power Spectral Density (PSD) of different implementations of Single-Carrier Frequency Division Multiple Access (SC-FDMA) are investigated. First, a general model of spectrally shaped SC-FDMA transmission scheme is proposed. This scheme is shown to encompass different implementations of SC-FDMA including the classical Long Term Evolution (LTE) SC-FDMA waveform. Then analytical expressions of PSD are derived for both localised and interleaved FDMA using or not spectral shaping techniques based on the aforementioned general SC-FDMA system model. Finally, analytical results are validated through comparison with simulation estimated PSD.

1. INTRODUCTION

New generation mobile networks such as LTE- Evolved Universal Terrestrial Radio Acess (EUTRA) require both low latency and high speed data conveying. However, the mobile radio channel suffers from Inter-Symbol Interference due to different fading phenomena arising from multipath propagation. A natural solution to the frequency selectivity of the channel is to use multi-carrier transmission schemes, such as FDMA. Yet, unlike single carrier transmissions, the fluctuations of multi-carrier signals lead to high Peak to Average Power Ratio (PAPR). This implies using a back-off to the saturation power of terminals amplifiers. Thus, energy consumption is degraded and the system is not attractive in terms of battery autonomy of the User Equipments (UE). Consequently, candidates to LTE uplink physical layer needed to have low PAPR which is the case of SC-FDMA also referred to as Discrete Fourier Transform (DFT)-spread OFDMA [1]. SC-FDMA is based on a DFT precoding of OFDM symbols, which ensures lower PAPR compared to OFDMA. There are two types of SC-FDMA systems differing in the way DFT outputs are mapped into the sub-carriers. The Localised SC-FDMA which is referred to as LFDMA, consists of mapping the DFT outputs into a block of consecutive sub-carriers. This mapping is the one chosen in LTE. A second mapping called Distributed FDMA, distributes the DFT outputs into sub-carriers over the entire bandwidth and when the spacing between subcarriers is constant it is called Interleaved FDMA. IFDMA has lower PAPR than LFDMA. However, IFDMA has not been selected by LTE standard since a fine synchronisation of all users is required, which is highly complex for multiple access networks. Even though having lower PAPR than OFDMA, reduction of SC-FDMA PAPR is still a highly desired feature. Many studies have been dedicated to further PAPR reduction. Some of the proposed solutions were directly inspired by the existing OFDM PAPR reduction techniques such as companding [2] and pulse shaping in the time domain [3]. Other solutions are based on pulse shaping in the frequency domain, commonly called Spectrum Shaping (SS) [4] [5] or more generally precoding [6]. Spectrum Shaping reduces the PAPR by windowing the DFT outputs before being mapped onto sub-carriers.

However, to the authors' knowledge, no thorough analysis of the power spectral density of SS-SC-FDMA systems has been presented in literature. Yet, knowing the spectral density is of paramount importance for users subcarrier allocation [7] as well as for fitting into the assigned transmission mask. OFDM PSD analytical expressions [8] are no longer valid because of the DFT precoding and spectral shaping. Hence, we need to develop a system model that would allow for a general abstraction of different spectrally shaped SC-FDMA implementations. We actually show that this general model encompasses all versions of mappings and spectral shaping functions of SC-FDMA and derive general analytical PSD. These results are compared with estimated spectral densities of different SC-FDMA implementations.

This paper is outlined as follows. Section 2 presents the generalised spectral shaping transmitter model which allows us to develop theoretical results of PSD in section 3 and some comparisons with simulation results. In section 4, we derive the PSD of IFDMA with spectral shaping before ending with some remarks and conclusion. In the following, the term x-DFT (resp. y-IDFT) designates a DFT over x points and IDFT over y points respectively.

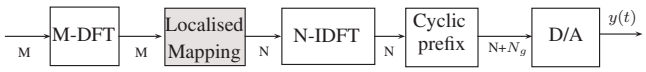

Fig. 1. Classical LFDMA

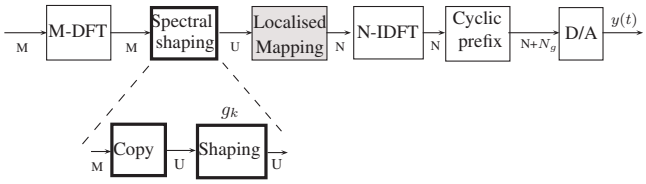

Fig. 2. LFDMA with spectral shaping $M \leq U \leq 2M$

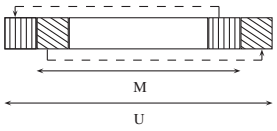

Fig. 3. Copying: Increasing length from M to U

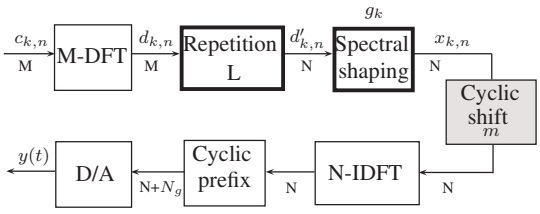

Fig. 4. LFDMA with general spectral shaping $U = N$

2. SPECTRALLY SHAPED LFDMA

All following results assume a mono-user scheme. A classical localised FDMA scheme is depicted in Fig. 1. It consists of M-DFT precoding of input symbols and mapping these outputs into contiguous M out of the N-IDFT inputs.

Spectrally shaped LFDMA in Fig. 2 consists of an additional (Spectrum Shaping) block at the output of the M-DFT which is an element wise multiplication with some specific frequency domain response of U samples. Since U can be larger than M, the M-DFT outputs need to be extended to reach a length of U symbols. This operation is done by copying as depicted in Fig. 3. The Copy block has been proposed in [4] considering that $M \leq U \leq 2M$ for raised cosine spectral shaping. However, in order to account for general spectral shapes of length U up to N, we replace the copying block by an L-fold repetition where $L = N/M$ is the SC-FDMA spreading factor (i.e. the maximum allowed number of users for N sub-carriers).

Hence, we derive the general physical model of SS-LFDMA as depicted in Fig. 4: blocks of M zero mean independent identically distributed (i.i.d) data symbols $c_{k,n}$ drawn from a complex alphabet of duration T_c are M-DFT precoded. The notation $(.)_{k,n}$ indicates the symbol on the k^{th} sub-carrier for the n^{th} SC-FDMA time domain symbol. An L-fold repetition allows transforming the M symbols into N symbols $d'_{k,n}$ which are then frequency shaped by a general transfer function of N samples (g_k). The N resulting symbols $x_{k,n} = d'_{k,n} g_k$ are then cyclically shifted by m samples to fit in the user's allocated sub-carrier indexes beginning at position m. Notice that the cyclic shift does the same role as spectral mapping in classical LFDMA, except that here the signals to be mapped have length N, which explains why we resort to cyclic shifting to map the symbols into the N-IDFT entries. In order to allow for flexible spectral mapping, m is not necessarily supposed multiple of M. After N-IDFT processing, a cyclic prefix of length N_g is appended to the beginning of each block n of length N. The output samples are then passed through an ideal digital to analog converter. The duration of the block n becomes $T = T_s + T_g$, where $T_s = NT_c$ is the SC-FDMA symbol duration and $T_g = N_g T_c$ is the cyclic prefix duration.

It should be noted that the original LTE SC-FDMA waveform is a special case of the general spectrally shaped LFDMA, where the shaping filter is a rectangular window of length M beginning at index 0 as depicted in Fig. 5. In this case, the combination of repetition, rectangular shaping and cyclic shift is equivalent to the sub-carrier mapping presented in LTE classical SC-FDMA.

When a raised cosine (RC) spectral shaping with a nonzero roll-off is used, the outputs of the spectral shaping have more than M non zero elements as depicted in Fig.6.

3. PSD OF GENERAL SPECTRALLY SHAPED LFDMA

For the following theoretical results, no hypothesis about the spectral shaping coefficients g_k are made. The transmitter output signal $y(t)$ can be expressed as follows :

$$y(t) = \frac{1}{N} \sum_{n=-\infty}^{\infty} \sum_{k=0}^{N-1} x_{k,n} e^{2j\pi < k+m >_N \Delta f (t-nT_g)} h(t-nT) \tag{1}$$

where $\Delta f = 1/T_s$ is the sub-carrier spacing, $h(t)$ is a rectangular function with duration T and $< a >_N$ designates a modulo N for $a \in \mathbb{Z}$. Taking into account that the outputs $d'_{k,n} = d_{<k>_N,n}$, the signal $y(t)$ can be simplified as follows:

$$\begin{aligned} y(t) &= \frac{1}{N} \sum_{n=-\infty}^{\infty} \sum_{k=0}^{N-1} x_{k,n} e^{2j\pi < k+m >_N \Delta f (t-nT_g)} h(t-nT) \\ &= \frac{1}{N} \sum_{n=-\infty}^{\infty} \sum_{k=0}^{N-1} d'_{k,n} g_k e^{2j\pi < k+m >_N \Delta f (t-nT_g)} h(t-nT) \\ &= \sum_{n=-\infty}^{\infty} \sum_{r=0}^{M-1} d_{r,n} g_r^{(m)} (t-nT) \end{aligned} \tag{2}$$

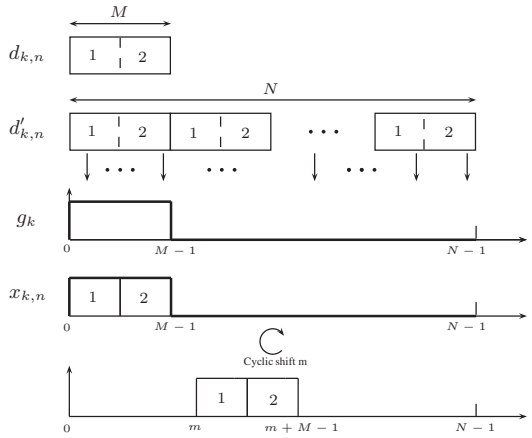

Fig. 5. LFDMA waveform with rectangular spectral shaping

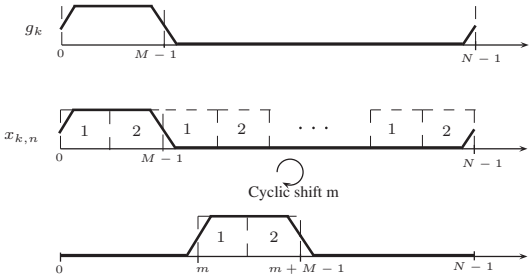

Fig. 6. Raised cosine spectral shaping output

where the last equality results from the Euclidean division of k as $pM + r$ with $p = 0, \cdots, L-1$ and $r = 0, \cdots, M-1$, and where we define the equivalent filters $g_r^{(m)}(t)$ as :

$$g_r^{(m)}(t) = \sum_{p=0}^{L-1} g_{pM+r} e^{2j\pi < r+pM+m >_N \Delta f t} h(t) \qquad (3)$$

In order to compute the PSD of $y(t)$, the statistical properties of the M-DFT outputs $d_{k,n}$ are needed. Since $d_{k,n}$ are the M-DFT outputs for the i.i.d inputs $c_{k,n}$, we have $d_{k,n} = \sum_{p=0}^{M-1} c_{p,n} e^{-\frac{2j\pi kp}{M}}$. The inter-correlation of the zero-mean symbols $d_{k,n}$ where $k = 0, \cdots, M-1$ satisfies:

$$\begin{aligned} E[d_{k,n} d^*_{k',n'}] &= \sum_{p=0}^{M-1} \sum_{p'=0}^{M-1} E[c_{p,n} c^*_{p',n'}] e^{-\frac{2j\pi(kp-k'p')}{M}} \\ &= \begin{cases} M\sigma_c^2 & if \;\; k = k' \;\; n = n' \\ 0 & elsewhere \end{cases} \end{aligned} \qquad (4)$$

where $\sigma_c^2 = E[|c_{p,n}|^2] \; \forall p, \; n$ is the variance of the zero mean input symbols $c_{p,n}$. It follows that the output of the M-DFT block are uncorrelated with variance $\sigma_d^2 = M\sigma_c^2$.
Let $R_{yy}(t,\tau)$ be the autocorrelation function of $y(t)$ defined as follows :

$$\begin{aligned} R_{yy}(t,\tau) &= E[y(t)y^*(t-\tau)] \\ &= \frac{1}{N^2} \sum_{n=-\infty}^{\infty} \sum_{r=0}^{M-1} \sum_{n'=-\infty}^{\infty} \sum_{r'=0}^{M-1} E[d_{r,n} d^*_{r',n'}] \\ &\quad g_r^{(m)}(t-nT) g_{r'}^{*(m)}(t-\tau-n'T) \\ &= \frac{M\sigma_c^2}{N^2} \sum_{n=-\infty}^{\infty} \sum_{r=0}^{M-1} g_r^{(m)}(t-nT) g_r^{*(m)}(t-\tau-nT) \end{aligned}$$

The expectation and autocorrelation of the signal $y(t)$ verify $E[y(t)] = 0$ and $R_{yy}(t,\tau)$ is T-periodic in t. Thus $y(t)$ is cyclo-stationary and we can define a stationarized autocorrelation function $\overline{R}_{yy}(\tau)$ as :

$$\begin{aligned} \overline{R}_{yy}(\tau) &= \frac{1}{T} \int_0^T R_{yy}(t,\tau) dt \\ &= \frac{M\sigma_c^2}{N^2 T} \sum_{r=0}^{M-1} \int_{-\infty}^{\infty} g_r^{(m)}(t) g_r^{*(m)}(t-\tau) dt \\ &= \frac{M\sigma_c^2}{N^2 T} \sum_{r=0}^{M-1} R^{(m)}_{g_r g_r}(\tau) \end{aligned} \qquad (5)$$

where $R^{(m)}_{g_r g_r}(\tau) = \int_{-\infty}^{\infty} g_r^{(m)}(t) g_r^{*(m)}(t-\tau) dt$ is the autocorrelation function of the equivalent filters $g_r^{(m)}(t)$.
Thus, the power spectral density of $y(t)$, which is the Fourrier Transform of the autocorrelation function $\overline{R}_{yy}(\tau)$, can be written as follows :

$$S_{yy}(f) = \mathcal{FT}\left(\overline{R}_{yy}(\tau)\right) = \frac{M\sigma_c^2}{N^2 T} \sum_{r=0}^{M-1} |G_r^{(m)}(f)|^2 \qquad (6)$$

where $G_r^{(m)}(f) = \sum_{p=0}^{L-1} g_{pM+r} H(f - < r + pM + m >_N \Delta f)$ are the transfer functions of filters $g_r^{(m)}(t)$.

3.a. Application to LFDMA with rectangular spectrum shaping

In this section, we are interested in the PSD of the classical LFDMA waveform, which consists of a rectangular spectral shaping with a response of length M as previously explained in Fig. 5. We suppose that the user allocated frequencies are at indexes $lM, \cdots, (l+1)M-1$. In this case, the spectrum shaping coefficients verify $g_k = 1$ if $k = 0, \cdots, M-1$ and 0 else. The samples $x_{k,n}$ are right-hand cyclically shifted by $m = lM$ in order to fit into indexes $lM, \cdots, (l+1)M-1$. The output filter transfer functions can be simplified to:

$$G_r^{(lM)}(f) = g_r H(f - < r + lM >_N \Delta f) \forall r = 0, \cdots, M-1 \qquad (7)$$

In order to compare the results of (7) and (6) with the simulated PSD of an LFDMA signal, we need to point out, as noted in [8], that the true frequency transfer function of a digital (sampled) rectangular function of length N is a Dirichlet

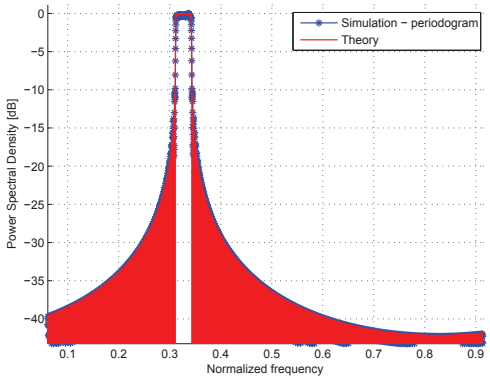

Fig. 7. LFDMA power spectral density for rectangular spectral shaping (N=512, M=16)

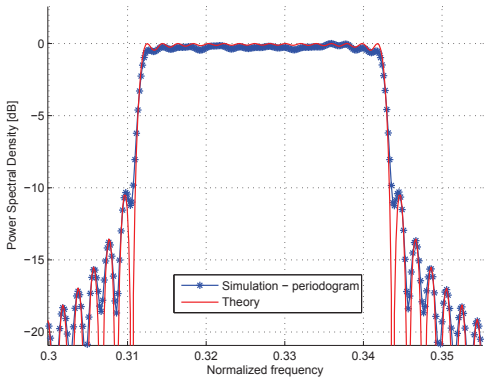

Fig. 8. Zoom on the central lobe of LFDMA power spectral density for rectangular spectral shaping (N=512, M=16)

kernel given by:

$$sinc_N(w) = \begin{cases} -1^{w(N-1)} & if\ w \in \mathbb{Z} \\ \frac{sin(Nw/2)}{Nsin(w/2)} & otherwise \end{cases} \quad (8)$$

As such, the transfer function of the simulated sampled rectangular function of length $N + N_g$ is $H(f) = (N + Ng)sinc_{N+Ng}(2\pi f)$.
Fig. 7 plots the obtained PSD for the classical LFDMA system with $N = 512$, $M = 16$, $m = 10M$ and $N_g = 0$. The LFDMA transmitter is based on the original LTE LFDMA scheme. The simulated PSD was obtained using a Welch periodogram estimator. A zoom on the central lobe of the PSD in Fig. 8 shows a good match between the simulated and theoretical curves.

3.b. Application to LFDMA with raised cosine spectrum shaping

In this section, we are interested in computing the PSD of LFDMA where a raised cosine spectral shaping with roll-off

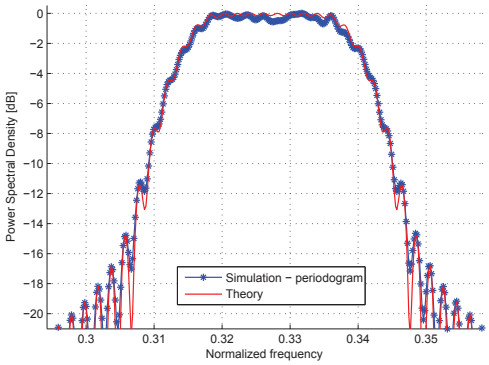

Fig. 9. Zoom on the central lobe of LFDMA power spectral density for raised cosine spectral shaping with ($\alpha = 0.5$, N=512, M=16)

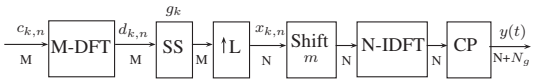

Fig. 10. SS-IFDMA system model

α is applied. Let $M_\alpha = \lfloor \alpha \frac{M}{2} \rfloor$ where $\lfloor . \rfloor$ denotes the floor operator. Since $0 \leq \alpha \leq 1$, the number of non zero shaping coefficients varies between M and $2M$. More specifically, the shaping coefficients g_k verify :

$$g_k \begin{cases} \neq 0 & if\ k = \{0, \cdots, M + M_\alpha - 1\} \cup \{N - M_\alpha, \cdots, N - 1\} \\ = 0 & else \end{cases}$$

Fig. 6 shows the outputs $x_{k,n}$ with a raised cosine spectral shaping before being shifted to the assigned frequency indexes. The frequency responses of the equivalent filters can be simplified as in (9).
Fig. 9 shows obtained PSD for the LFDMA system with RC spectrum shaping using a roll-off $\alpha = 0.5$ and the same other parameters as in the previous section. Again, there is a good match between simulated and theoretical curves.

4. PSD OF SPECTRALLY SHAPED IFDMA

IFDMA is an SC-FDMA variant based on an interleaved spectral mapping of the user's symbols. Let us consider the SS-IFDMA waveform depicted in Fig. 10. We shall restrict our analysis to the case where the length of the spectral shaping window does not exceed M. SS-IFDMA actually consists of upsampling the spectrally shaped M-DFT outputs by a factor L followed by a frequency shift m to meet the user's assigned frequencies at indexes $pL + m$ where $p = 0, \cdots, M - 1$. Again the classical IFDMA is a special case of SS-IFDMA, where spectrum shaping is a rectangular window of length M. This results in a new decomposition of the N-IDFT output signal $y(t)$ as:

$$y(t) = \frac{1}{N} \sum_{n=-\infty}^{\infty} \sum_{r=0}^{M-1} g_r d_{r,n} e^{2j\pi(rL+m)\Delta f(t-nT_g)} h(t - nT)$$

$$G_r^{(m)}(f) = \begin{cases} g_r H(f - < r+m >_N \Delta f) + g_{M+r} H(f - < M+r+m >_N \Delta f) & if\ r = 0, \cdots, M_\alpha - 1 \\ g_r H(f - < r+m >_N \Delta f) & if\ r = M_\alpha, \cdots, M - M_\alpha - 1 \\ g_r H(f - < r+m >_N \Delta f) + g_{(L-1)M+r} H(f - < (L-1)M+r+m >_N \Delta f) & if\ r = M - M_\alpha, \cdots, M-1 \end{cases} \quad (9)$$

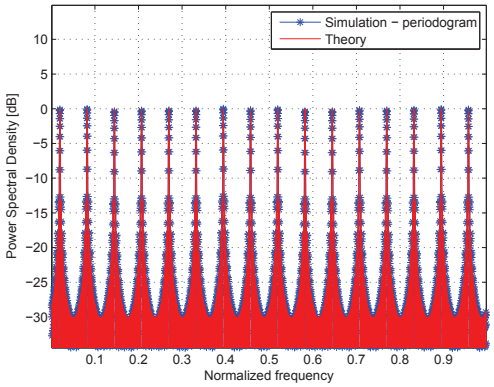

Fig. 11. IFDMA power spectral density (N=512, M=16)

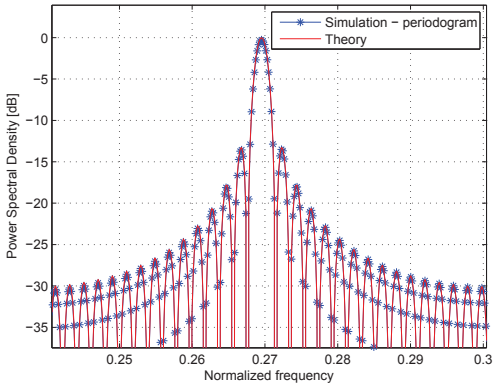

Fig. 12. Zoom on the central lobe of IFDMA power spectral density (N=512, M=16)

The stationarized autocorrelation $R_{yy}(\tau)$ of $y(t)$ is derived following the same steps as in section 3:

$$\overline{R}_{yy}(\tau) = \frac{M\sigma_c^2}{N^2 T} \sum_{r=0}^{M-1} |g_r|^2 e^{2j\pi(rL+m)\Delta f \tau} R_{hh}(\tau) \quad (10)$$

where $R_{hh}(\tau) = \int_{-\infty}^{\infty} h(t)h^*(t-\tau)dt$.
Thus, the PSD of the SS-IFDMA signal can be written as follows:

$$S_{yy}(f) = \frac{M\sigma_c^2}{N^2 T} \sum_{r=0}^{M-1} |g_r H(f - (rL+m)\Delta f)|^2 \quad (11)$$

Fig. 11 and Fig. 12 show the spectrum of classical IFDMA i.e. using a spectrum shaping satisfying $g_k = 1\, \forall k = 0, \cdots, M-1$. We observe a good match between theoretical and simulated PSD.

5. CONCLUSION

This paper presented a general model of spectrally shaped SC-FDMA system. The proposed model has the advantage of a high flexibility in the representation of different implementations of spectral shaping either for LFDMA or for IFDMA. Based on this model, we derived analytical expressions of PSD of spectrally shaped SC-FDMA schemes including the classical non spectrally shaped schemes. The analytical expressions were drawn for a single user but can be easily extended to the general case of multiple independent users.

6. REFERENCES

[1] Hyung G. Myung, Junsung Lim, and David J. Goodman, "Single carrier FDMA for uplink wireless transmission," *IEEE Vehicular Technology Magazine*, vol. 1, no. 3, pp. 30 –38, 2006, sept.

[2] Enchang Sun, Ruizhe Yang, Pengbo Si, Yanhua Sun, and Yanhua Zhang, "Raised Cosine-like companding scheme for peak-to-average power ratio reduction of SCFDMA signals," in *Global Mobile Congress (GMC)*, 2010, Oct., pp. 1–5.

[3] C.A. Azurdia-Meza, Kyujin Lee, and Kyesan Lee, "PAPR Reduction in SC-FDMA by Pulse Shaping Using Parametric Linear Combination Pulses," *IEEE Communications Letters*, vol. 16, no. 12, pp. 2008–2011, December.

[4] T. Kawamura, Y. Kishiyama, K. Higuchi, and M. Sawahashi, "Investigations on Optimum Roll-off Factor for DFT-Spread OFDM Based SC-FDMA Radio Access in Evolved UTRA Uplink," in *3rd International Symposium on Wireless Communication Systems, ISWCS '06.*, 2006, sept, pp. 383 –387.

[5] S. Adhikari, S.L. Jansen, M. Kuschnerov, O. Gaete, B. Inan, M. Bohn, and W. Rosenkranz, "Analysis of Spectral Shaping on DFT-OFDM," *IEEE Photonics Technology Letters*, vol. 25, no. 3, pp. 287–290, 2013, Feb.1.

[6] Guoliang Chen, S. H. Song, and K.B. Letaief, "A low-complexity precoding scheme for papr reduction in sc-fdma systems," in *IEEE Wireless Communications and Networking Conference (WCNC)*, 2011, pp. 1358–1362.

[7] B. Aziz, I. Fijalkow, and M. Ariaudo, "Trade off between frequency diversity and robustness to carrier frequency offset in uplink ofdma system," in *IEEE Global Telecommunications Conference (GLOBECOM 2011)*, 2011, pp. 1–5.

[8] T. van Waterschoot, V. Le Nir, J. Duplicy, and M. Moonen, "Analytical Expressions for the Power Spectral Density of CP-OFDM and ZP-OFDM Signals," *IEEE Signal Processing Letters*, vol. 17, no. 4, pp. 371–374, 2010, April.